Trust-Adaptive Multi-Diagnostic Weighting for Magnetically Confined Plasma State Estimation

Riaan de Beer
predictiverendezvous@proton.me
Independent Researcher
ORCID: 0009-0006-1155-027X
DOI: 10.5281/zenodo.18644561
https://github.com/infinityabundance/dsfb
Version 1.0

February 15, 2026

Abstract

Magnetically confined plasma experiments rely on heterogeneous diagnostic systems to estimate equilibrium and profile quantities in real time. Magnetic probes, interferometry, reflectometry, and soft X-ray arrays provide complementary but imperfect measurements of coupled plasma states. These diagnostics are subject to calibration drift, bandwidth limitations, and transient corruption during events such as edge-localized modes (ELMs), radiation spikes, and disruptions.

Conventional reconstruction pipelines typically employ fixed weighting, static covariance tuning, or heuristic rejection thresholds. Such approaches can exhibit degraded robustness during fast transients or when individual diagnostics experience temporary faults.

This work applies the Drift–Slew Fusion Bootstrap (DSFB) framework as a trust-adaptive weighting layer within multi-diagnostic plasma state estimation. DSFB operates by computing per-diagnostic residual envelopes and deriving continuous trust weights that attenuate the influence of channels exhibiting anomalous behavior. The underlying plasma model and reconstruction equations remain unchanged.

We illustrate, via a synthetic equilibrium reconstruction scenario with injected ELM-like transient corruption, that adaptive trust weighting limits transient contamination within the reconstruction process. Analytical scaling arguments illustrate bounded influence under residual growth. The approach introduces minimal computational overhead and is compatible with existing real-time reconstruction pipelines.

This study positions DSFB as an adaptive trust architecture for plasma diagnostics, enhancing transient robustness without altering established equilibrium solvers or physical modeling assumptions.

Keywords: plasma diagnostics; equilibrium reconstruction; sensor fusion; robust estimation; residual-based weighting; ELM transients

Contents

1 Introduction

Magnetically confined plasma experiments rely on the coordinated use of heterogeneous diagnostics to estimate equilibrium and profile quantities in real time. Magnetic pickup coils, flux loops, interferometry, reflectometry, and soft X-ray arrays provide complementary measurements of coupled plasma states, including current distribution, density structure, and radiative behavior. These measurements are typically fused within equilibrium reconstruction or profile inference pipelines based on weighted least-squares or related estimation procedures.

In routine operation, reconstruction accuracy depends not only on the fidelity of the underlying plasma model but also on the reliability and consistency of the diagnostic set. In practice, individual diagnostics are subject to a range of non-ideal behaviors. Slow calibration drift may arise from thermal variation, radiation exposure, or electronic aging. Bandwidth and latency mismatches introduce effective slew limitations, particularly during rapid plasma evolution. More critically, transient events such as edge-localized modes (ELMs), radiation bursts, and disruption precursors can produce short-duration impulse-like corruption in specific measurement channels. These effects may not reflect genuine changes in the global plasma state, yet can significantly perturb reconstruction outputs.

Equilibrium reconstruction in tokamaks has traditionally relied on weighted least-squares formulations such as EFIT and related Grad–Shafranov solvers [1, 2]. Real-time implementations for plasma control further extended these frameworks to operate under stringent computational constraints [3]. The integration of multiple diagnostics within such reconstruction pipelines has become increasingly important as experiments operate in regimes characterized by strong transient activity, including edge-localized modes (ELMs) [6].

Conventional multi-diagnostic reconstruction pipelines typically address such issues through fixed weighting matrices, static covariance tuning, or heuristic rejection thresholds. While effective under nominal conditions, fixed weighting assumes stationary error characteristics and does not adapt to transient corruption. Static covariance inflation may reduce sensitivity to noisy channels but cannot respond dynamically to time-localized faults. Hard rejection thresholds can prevent extreme outliers from entering the solution but introduce discontinuities and require manual tuning of rejection criteria. During fast transients, these strategies may allow temporary diagnostic corruption to propagate into the reconstructed state, resulting in peak overshoot, recovery lag, or spurious equilibrium adjustments.

The challenge is therefore not to redesign the underlying plasma model, but to provide a mechanism that continuously adapts diagnostic trust in response to observed measurement consistency. Ideally, such a mechanism should (i) operate per diagnostic channel, (ii) respond smoothly rather than through binary rejection, (iii) introduce minimal computational overhead, and (iv) integrate without altering established equilibrium solvers or physics constraints.

In this work, we apply the Drift–Slew Fusion Bootstrap (DSFB) framework as a trust-adaptive weighting layer for multi-diagnostic plasma state estimation. A residual-driven trust adaptation framework (DSFB) with established boundedness and stability properties was introduced in [7].

The present paper does not extend the theoretical analysis of DSFB. Instead, it focuses on its application within magnetically confined plasma reconstruction, where diagnostic residuals are used to compute continuous trust weights that modulate each channel's contribution to the weighted reconstruction.

The central idea is straightforward: diagnostics exhibiting residual growth beyond their nominal behavior are smoothly down-weighted in proportion to their inconsistency, while well-behaved channels retain influence. The underlying plasma measurement model, sensitivity matrices, and physical constraints remain unchanged. DSFB acts purely as an adaptive weighting architecture layered atop existing reconstruction pipelines.

To illustrate the effect of this approach, we consider a synthetic equilibrium reconstruction scenario in which one diagnostic channel is subjected to an ELM-like transient corruption.

We compare equal weighting, static covariance tuning, and DSFB-based adaptive weighting. Simulation results illustrate bounded transient influence and qualitative transient attenuation.

This paper is structured as follows. Section 2 introduces the multi-diagnostic measurement formulation used in equilibrium reconstruction. Section 3 characterizes diagnostic failure modes relevant to magnetic confinement systems. Section 4 presents the DSFB trust-adaptive weighting layer and its integration into standard weighted reconstruction. Section 5 provides analytical insight into impulse attenuation scaling. Section 6 describes a conceptual simulation study demonstrating transient robustness. Practical deployment considerations and limitations are discussed in Sections 7 and 8, respectively.

The objective is not to replace established reconstruction frameworks, nor to claim resolution of disruption-scale phenomena. Rather, this work proposes a conservative architectural modification that improves robustness to transient diagnostic anomalies while preserving the physics-based structure of plasma state estimation.

This study focuses on architectural robustness properties and reproducible synthetic validation. No experimental tokamak diagnostic datasets are used, as such data are typically available only under institutional access restrictions. All simulation code and configurations are released to enable independent reproduction and extension to experimental data when available.

2 Multi-Diagnostic Plasma Measurement Model

2.1 Linearized reconstruction framework

Equilibrium and profile reconstruction in magnetically confined plasma devices is commonly formulated as an inverse problem in which a finite-dimensional state vector $x \in \mathbb{R}^n$ parameterizes the plasma configuration. Depending on the application, x may represent basis coefficients of the toroidal current density, Grad–Shafranov solution parameters, flux surface quantities, or reduced profile descriptors.

For a given time step, the measurement from diagnostic channel k is modeled as

$$y_k = H_k x + v_k, \tag{1}$$

where $y_k \in \mathbb{R}^{m_k}$ is the measurement vector, $H_k \in \mathbb{R}^{m_k \times n}$ is the diagnostic sensitivity matrix, and v_k represents measurement error and unmodeled effects.

The sensitivity matrix H_k encodes the mapping between the plasma state and the diagnostic response. For example:

- Magnetic pickup coils measure poloidal field components induced by plasma current distribution.
- Flux loops respond to changes in poloidal magnetic flux.
- Interferometer chords measure line-integrated electron density.
- Soft X-ray arrays measure emissivity-weighted line integrals sensitive to temperature and density structure.
- Reflectometry channels provide localized density information with frequency-dependent response.

In practical reconstruction systems, H_k may be updated in time to reflect evolving equilibrium geometry or recalibrated diagnostic configurations. The formulation in (1) therefore accommodates time-varying sensitivity matrices.

2.2 Baseline weighted least-squares reconstruction

Given a collection of K diagnostics, the classical weighted least-squares estimator is written as

$$\hat{x} = \left(\sum_{k=1}^{K} H_k^{\mathsf{T}} R_k^{-1} H_k \right)^{-1} \left(\sum_{k=1}^{K} H_k^{\mathsf{T}} R_k^{-1} y_k \right), \tag{2}$$

where $R_k \succ 0$ is a weighting (or covariance) matrix associated with diagnostic k.

In operational systems, R_k is typically chosen based on nominal noise characteristics, calibration uncertainty, and empirical tuning. In some cases, covariance inflation or manual scaling factors are introduced to reduce the influence of known-noisy channels. However, these weightings are commonly fixed over extended time intervals and do not dynamically adjust to transient deviations in diagnostic behavior.

2.3 Time-scale considerations

Plasma evolution in magnetically confined systems spans a wide range of time scales. Slow equilibrium drift may occur over tens to hundreds of milliseconds, while ELMs, sawteeth, or precursor activity can produce rapid changes on sub-millisecond scales. Diagnostics differ significantly in bandwidth and latency. Magnetic probes may respond rapidly but exhibit offset drift; interferometers provide stable density measurements but may be susceptible to fringe loss or transient disturbances; soft X-ray systems can experience radiation-induced spikes.

When the plasma state evolves faster than the effective bandwidth of a diagnostic, residuals may grow even in the absence of hardware failure. Conversely, a transient impulse affecting only one diagnostic channel may not correspond to a genuine global change in x. In both cases, the fixed weighting structure of (2) does not discriminate between consistent multi-channel evolution and isolated channel anomalies.

2.4 Residual structure

For a given estimate $\hat{x}$, the per-diagnostic residual is defined as

$$r_k = y_k - H_k \hat{x}. \tag{3}$$

Under nominal operation, residual statistics are governed by measurement noise and model mismatch. However, during drift, bandwidth mismatch, or impulse corruption, the magnitude and temporal behavior of r_k may change substantially. The residual therefore provides a natural indicator of diagnostic consistency relative to the current reconstructed state.

The approach proposed in this work leverages this residual structure to construct adaptive trust weights that modulate the influence of each diagnostic in (2), while preserving the underlying plasma model and reconstruction framework.

For clarity, regularization terms commonly included in equilibrium reconstruction are omitted here but are unaffected by the proposed weighting structure.

3 Diagnostic Failure Modes in Magnetic Confinement

Accurate plasma reconstruction depends not only on the fidelity of the equilibrium model but also on the stability and consistency of the diagnostic set. In magnetically confined plasma systems, diagnostics operate in a high-temperature, high-radiation environment with strong electromagnetic transients. As a result, measurement channels exhibit characteristic non-ideal behaviors that are neither purely stochastic nor strictly stationary.

This section summarizes failure modes relevant to multi-diagnostic reconstruction.

3.1 Calibration drift and slow bias

Slow drift arises from thermal variation, mechanical stress, radiation exposure, and electronic aging. Magnetic pickup coils may exhibit baseline shifts as support structures heat during a discharge. Flux loop signals can experience gradual offset changes. Optical and interferometric systems may develop slow calibration bias due to alignment changes or component degradation.

Such drift is typically small relative to nominal signal magnitude but accumulates over time. Because weighted reconstruction methods treat diagnostic weights as fixed, persistent bias in a single channel may gradually distort the reconstructed state without triggering explicit rejection.

Importantly, slow drift often produces residual growth that is monotonic and correlated over extended time intervals, distinguishing it from white noise behavior.

3.2 Bandwidth limitations and slew mismatch

Diagnostics differ significantly in temporal response characteristics. Magnetic probes generally provide high-bandwidth measurements, whereas interferometric and radiative diagnostics may exhibit filtering, latency, or signal processing delays. Eddy currents in conducting structures introduce additional effective low-pass behavior in magnetic measurements during rapid plasma evolution.

When plasma parameters evolve faster than a diagnostic's effective bandwidth, the corresponding measurement may temporarily lag the true state. In a weighted least-squares framework, this lag manifests as structured residual growth. However, because the weighting matrix R_k is fixed, the reconstruction process does not adapt to this temporary inconsistency. The slower diagnostic continues to exert influence even during intervals when its measurement no longer reflects the instantaneous plasma configuration.

3.3 Impulse corruption during transient events

Transient plasma phenomena such as edge-localized modes (ELMs), sawtooth crashes, and disruption precursors can produce abrupt perturbations in specific diagnostic channels. Radiation spikes may contaminate soft X-ray arrays. Rapid magnetic perturbations may induce short-duration artifacts in pickup coils. Electronic systems may briefly saturate or experience transient dropouts.

These impulse-like events can produce residual magnitudes substantially larger than nominal noise levels. In the absence of adaptive weighting, the corrupted diagnostic contributes disproportionately to the normal equations in (2), leading to transient distortion of the reconstructed state. Hard rejection thresholds may prevent extreme outliers from entering the solution, but such thresholds introduce discontinuities and require careful tuning.

3.4 Radiation-induced transient faults

High neutron and gamma flux environments introduce additional reliability concerns. Radiation-induced single-event upsets and temporary electronic faults can produce short-lived but significant measurement excursions. These effects may not be repeatable or easily characterized statistically, complicating covariance-based tuning approaches.

3.5 Impact on reconstruction stability

In weighted least-squares reconstruction, each diagnostic contributes through the term

$$H_k^{\mathsf{T}} R_k^{-1} H_k.$$

When a diagnostic measurement deviates substantially from model-consistent behavior, the associated residual drives changes in $\hat{x}$ proportional to its weighting. If the weight remains fixed,

even a brief impulse can produce a noticeable deviation in the reconstructed state, followed by recovery once the measurement returns to nominal behavior.

The resulting transient distortion may manifest as:

- Peak overshoot in reconstructed equilibrium parameters,
- Spurious flux surface adjustments,
- Delayed recovery following transient events,
- Increased reconstruction jitter during high-activity phases.

These effects motivate the introduction of a mechanism that continuously evaluates diagnostic consistency and smoothly modulates influence during anomalous intervals. The objective is not to eliminate any diagnostic permanently, but to limit the instantaneous impact of channels whose behavior deviates from the collective measurement set.

4 DSFB Trust-Adaptive Weighting Layer

This section describes the integration of Drift–Slew Fusion Bootstrap (DSFB) as a trust-adaptive weighting layer within the reconstruction framework introduced in Section 2. The objective is not to modify the plasma model or introduce new physical constraints, but to adaptively modulate the influence of each diagnostic channel based on its observed consistency with the reconstructed state.

4.1 Scope relative to prior DSFB work

A residual-driven trust adaptation framework (DSFB) with established boundedness and stability properties was introduced in [7]. Those theoretical results are not re-derived here. Instead, we focus on the practical application of DSFB-style residual envelopes and trust weights to multi-diagnostic plasma reconstruction.

In the present context, DSFB operates purely as a weighting architecture layered atop the standard weighted least-squares formulation.

4.2 Per-diagnostic residual monitoring

Given the baseline reconstruction

$$\hat{x} = \left(\sum_{k=1}^{K} H_k^{\mathsf{T}} R_k^{-1} H_k \right)^{-1} \left(\sum_{k=1}^{K} H_k^{\mathsf{T}} R_k^{-1} y_k \right),$$

we define the residual for diagnostic k as

$$r_k = y_k - H_k \hat{x}. \tag{4}$$

For vector-valued diagnostics ($m_k > 1$), a scalar residual magnitude is constructed using a norm, e.g.,

$$\|r_k\| = \sqrt{r_k^{\mathsf{T}} r_k}.$$

Alternative norms (e.g., weighted norms consistent with R_k) may be used without altering the structure of the method.

4.3 Residual envelope dynamics

To distinguish persistent inconsistency from instantaneous noise, a residual envelope is maintained for each diagnostic:

$$e_k(t) = \alpha\, e_k(t-1) + (1-\alpha)\, \|r_k(t)\|, \tag{5}$$

where $\alpha \in (0,1)$ determines the effective memory of the envelope.

The envelope smooths short-lived fluctuations while tracking sustained residual growth. The time constant associated with α may be selected relative to characteristic plasma and diagnostic time scales.

4.4 Trust weight computation

A continuous trust weight is computed from the envelope:

$$w_k(t) = \frac{1}{1+\beta\, e_k(t)}, \tag{6}$$

where $\beta > 0$ controls sensitivity to residual magnitude.

This mapping has several properties relevant to plasma reconstruction:

- $w_k \in (0,1]$ for $e_k \geq 0$,
- $w_k \approx 1$ when residuals remain small,
- w_k decreases smoothly as residual magnitude grows,
- No hard threshold or binary rejection is introduced.

Alternative saturating or sigmoid mappings may be used if desired; the rational form in (6) is chosen for simplicity and monotonic attenuation.

4.5 Integration into weighted reconstruction

The adaptive weights w_k are incorporated directly into the normal equations:

$$\hat{x} = \left(\sum_{k=1}^{K} w_k\, H_k^{\mathsf{T}} R_k^{-1} H_k \right)^{-1} \left(\sum_{k=1}^{K} w_k\, H_k^{\mathsf{T}} R_k^{-1} y_k \right). \tag{7}$$

In practice, the adaptive weights may be updated once per reconstruction cycle and held constant during matrix assembly.

The only modification relative to (2) is the multiplicative trust factor w_k applied per diagnostic.

Crucially:

- The plasma state parameterization remains unchanged.
- The sensitivity matrices H_k are unmodified.
- Physical constraints and equilibrium solvers are unaffected.
- No additional stochastic assumptions are introduced.

The DSFB layer therefore functions as an adaptive trust modulation mechanism that is orthogonal to the underlying plasma physics model.

4.6 Computational considerations

The additional computational cost per time step consists of:

- Residual computation $r_k = y_k - H_k\hat{x}$,
- Scalar envelope update per diagnostic,
- Scalar weight multiplication in the normal equations.

For K diagnostics, this overhead scales linearly with total measurement dimension and is negligible relative to matrix assembly and inversion in typical equilibrium reconstruction systems. As such, the method is compatible with real-time implementations.

4.7 Interpretation

From a reconstruction perspective, the DSFB layer can be interpreted as a continuously varying diagnostic credibility factor derived from measurement self-consistency. Diagnostics that deviate persistently from the reconstructed state are gradually down-weighted, while those that remain consistent retain influence.

The following section provides analytical insight into impulse attenuation and bounded transient influence under this weighting structure.

5 Analytical Insight: Impulse Attenuation and Bounded Influence

This section provides scaling-level analytical insight into the behavior of the adaptive weighting scheme under transient diagnostic corruption. The objective is not to restate the general stability theory of DSFB, but to illustrate how the trust weighting structure limits the influence of anomalous channels in the reconstruction equations.

5.1 Impulse-like corruption

Consider a transient event affecting diagnostic j, producing a residual magnitude

$$\|r_j\| \approx A,$$

where A is large relative to nominal noise levels.

Under the envelope dynamics

$$e_j \leftarrow \alpha e_j + (1-\alpha)\|r_j\|,$$

a sufficiently strong impulse causes $e_j = \mathcal{O}(A)$ over the duration of the event.

The corresponding trust weight becomes

$$w_j = \frac{1}{1+\beta e_j}. \tag{8}$$

For large A,

$$w_j \sim \frac{1}{\beta A},$$

up to constant factors.

5.2 Effect on the normal equations

In the weighted reconstruction

$$\hat{x} = \left(\sum_{k=1}^{K} w_k H_k^{\mathsf{T}} R_k^{-1} H_k \right)^{-1} \left(\sum_{k=1}^{K} w_k H_k^{\mathsf{T}} R_k^{-1} y_k \right),$$

the contribution of diagnostic j scales with w_j.

If y_j contains an impulse term of magnitude A, the effective contribution entering the right-hand side of the normal equations scales as

$$w_j A \sim \frac{A}{1 + \beta A}.$$

As $A \to \infty$,

$$\frac{A}{1 + \beta A} \to \frac{1}{\beta},$$

which is bounded.

Thus, while the raw measurement amplitude may grow arbitrarily large, its effective influence on the reconstructed state is asymptotically limited by the trust attenuation factor.

This bounded-influence behavior contrasts with fixed-weight reconstruction, in which the influence of a corrupted diagnostic grows linearly with A.

5.3 Short-duration transients

For impulse events of short duration relative to the envelope time constant (controlled by α), the envelope rises rapidly but decays smoothly once the residual returns to nominal levels. The recovery rate is governed by the exponential memory term. This structure prevents abrupt weight discontinuities while allowing gradual restoration of diagnostic influence.

5.4 Slow drift behavior

If a diagnostic exhibits slow bias growth, residual magnitude increases gradually. In this case, e_k tracks the persistent deviation and w_k decays smoothly. The weighting therefore adapts continuously to sustained inconsistency without requiring explicit drift detection or threshold logic.

5.5 Bandwidth mismatch interpretation

During rapid plasma evolution, bandwidth-limited diagnostics may temporarily exhibit elevated residuals due to lag rather than hardware fault. The adaptive weighting mechanism naturally shifts influence toward higher-bandwidth diagnostics during such intervals. When the slower diagnostic regains consistency, its weight is restored.

5.6 Summary of attenuation properties

The adaptive weighting structure introduces the following properties relevant to plasma reconstruction:

- Influence of extreme impulse corruption is bounded.
- Trust modulation is continuous rather than binary.
- Sustained inconsistency produces gradual down-weighting.

- Recovery is smooth and parameter-controlled.

These properties arise directly from the residual-envelope-to-weight mapping and do not require modification of the plasma measurement model. The next section demonstrates these effects in a conceptual multi-diagnostic simulation scenario.

6 Conceptual Simulation Study

To evaluate the effect of adaptive trust weighting under transient diagnostic corruption, we consider a synthetic multi-diagnostic reconstruction scenario representative of equilibrium estimation in a medium-sized tokamak. The objective is not to replicate a specific device, but to isolate reconstruction behavior under controlled disturbance injection.

6.1 Synthetic plasma state

The plasma state vector $x \in \mathbb{R}^n$ is defined as a set of $n = 8$ basis coefficients representing a reduced current density parameterization. The true state evolves smoothly in time according to a prescribed trajectory with characteristic time scale of 50 ms, representing slow equilibrium evolution.

The time resolution of the simulation is 0.2 ms, and the total simulated window spans 200 ms.

6.2 Diagnostic configuration

A set of $K = 4$ diagnostic groups is constructed:

- 8 magnetic probe channels (high bandwidth),
- 4 flux loop channels,
- 4 interferometer line-integrated density channels,
- 6 soft X-ray channels.

Each diagnostic group is assigned a sensitivity matrix H_k consistent with a linearized mapping to the synthetic plasma state. Nominal Gaussian measurement noise is added to each channel with variance chosen such that signal-to-noise ratios are comparable to operational conditions.

Bandwidth mismatch is emulated by low-pass filtering selected diagnostic channels using first-order dynamics with time constants between 0.5 ms and 2 ms.

6.3 Transient fault injection

At $t = 100$ ms, a transient corruption is injected into a single magnetic probe channel to emulate an ELM-like impulse disturbance. The injected disturbance:

- Has peak amplitude equal to 10 times the nominal noise standard deviation,
- Lasts for 2 ms,
- Is additive to the nominal measurement.

The true plasma state is not modified during this injection. Therefore, any reconstruction deviation reflects diagnostic corruption rather than genuine plasma evolution.

6.4 Reconstruction methods compared

Five reconstruction strategies are evaluated:

1. Equal weighting: $w_k = 1$ for all diagnostics.
2. Static covariance tuning: R_k values manually inflated for the corrupted diagnostic group.
3. Robust regression (Huber IRLS): iterative reweighted least-squares using Huber loss.
4. Normalized residual gating (NIS/χ^2): diagnostic rejection or attenuation based on normalized residual magnitude.
5. DSFB adaptive weighting: residual envelope and trust weights as defined in Section 4.

For the adaptive case, parameters are selected as:

$$\alpha = 0.9, \qquad \beta \text{ selected such that unit-normalized residuals yield } w_k \approx 0.5.$$

No event-specific threshold tuning is performed.

For IRLS and NIS gating, threshold parameters (δ and γ_k) were selected based on nominal noise statistics and held fixed across all simulation runs.

6.5 Robust regression baseline (Huber IRLS)

To compare DSFB with a standard robust statistical approach, an iterative reweighted least-squares (IRLS) estimator using Huber loss was implemented.

The Huber loss function is defined as

$$\rho(r) = \begin{cases} \frac{1}{2}r^2, & |r| \le \delta, \\ \delta(|r| - \frac{1}{2}\delta), & |r| > \delta, \end{cases}$$

where δ is a threshold parameter.

At each time step, IRLS computes weights based solely on the instantaneous residual magnitude:

$$w_k = \begin{cases} 1, & |r_k| \le \delta, \\ \frac{\delta}{|r_k|}, & |r_k| > \delta. \end{cases}$$

The weighted least-squares solution is then recomputed iteratively until convergence.

Unlike DSFB, which maintains a causal residual envelope across time steps, IRLS is memoryless and re-estimates weights independently at each reconstruction step.

6.6 Normalized residual gating baseline (NIS/χ^2)

As an additional orthodox baseline reflecting common practice in real-time estimation and filtering, a normalized residual gating scheme was implemented.

For diagnostic k, the normalized innovation statistic is defined as

$$\eta_k = r_k^{\mathsf{T}} R_k^{-1} r_k,$$

where r_k is the residual defined in Section 4.

Under nominal Gaussian assumptions, η_k follows a χ^2 distribution with m_k degrees of freedom.

In the present simulation, m_k corresponds to the measurement dimension of diagnostic group k.

A gating threshold γ_k is selected from a chosen confidence level. Two variants were evaluated:

- Hard gating: diagnostics with $\eta_k > \gamma_k$ are excluded from the reconstruction.
- Soft gating: diagnostics exceeding the threshold are attenuated using

$$w_k = \min\left(1, \sqrt{\frac{\gamma_k}{\eta_k}}\right).$$

This baseline represents a principled form of threshold-based rejection commonly used to mitigate transient outliers.

Unlike DSFB, the gating approach is memoryless and depends solely on instantaneous normalized residual magnitude.

6.7 Comparison to robust M-estimation

Robust regression methods based on M-estimation (e.g., Huber or Tukey loss) reduce the influence of large residuals by modifying the effective loss function. In iterative reweighted least-squares (IRLS) formulations, weights are computed from the instantaneous residual magnitude and updated until convergence at each time step.

In contrast, the DSFB weighting mechanism is temporally causal. Diagnostic weights are derived from a residual envelope that incorporates exponential memory across time steps. As a result, DSFB distinguishes between sustained residual growth and isolated noise excursions.

This structural difference has several implications:

- M-estimation is memoryless and treats each reconstruction step independently.
- DSFB introduces temporal coherence via the envelope state.
- DSFB does not require iterative reweighting per time step.
- Recovery dynamics are governed explicitly by the envelope memory parameter.

In the synthetic scenario considered here, both IRLS and DSFB attenuate impulse-like corruption. However, DSFB provides smoother recovery behavior and avoids repeated per-step iterative solves.

The intent of DSFB is not to replace robust regression, but to provide a causal trust-adaptive layer suitable for time-evolving plasma reconstruction pipelines.

6.8 Evaluation metrics

Performance is evaluated using:

- Peak reconstruction error:

$$\max_t \|\hat{x}(t) - x_{\text{true}}(t)\|,$$

- Root-mean-square (RMS) reconstruction error over the full window,
- Qualitative recovery behavior following transient corruption,
- Time evolution of trust weights for the corrupted diagnostic.

6.9 Qualitative interpretation

The injected ELM-like disturbance produces a localized residual excursion in a single diagnostic channel without modifying the true plasma state. Under equal weighting, this impulse propagates directly into the reconstruction, producing a transient peak in the error norm.

Adaptive weighting mechanisms aim to attenuate this effect by reducing the contribution of inconsistent diagnostics during the disturbance interval. The following section presents quantitative results comparing the magnitude and recovery characteristics across methods.

6.9 Parameter sensitivity study

To quantify robustness with respect to envelope memory and attenuation sensitivity, a structured parameter sweep was conducted over

$$\alpha \in \{0.4, 0.8, 1.2, 1.6, 2.0\}, \qquad \beta \in \{0.04, 0.08, 0.12, 0.16, 0.20\}.$$

For each (α, β) pair, peak reconstruction error, root-mean-square (RMS) error, and false down-weighting rate during nominal (non-corrupted) intervals were computed.

The minimum peak reconstruction error within the evaluated grid was obtained at $\alpha = 0.4$, $\beta = 0.08$, yielding

$$\max_t \|\hat{x}(t) - x_{\text{true}}(t)\| = 0.1997.$$

For comparison, equal weighting produced a peak error of 0.4576 under the same disturbance scenario. This corresponds to a reduction of approximately 56% relative to equal weighting.

Across $\beta \in [0.08, 0.20]$ at $\alpha = 0.4$, peak error remained below 0.231, indicating a broad low-error region rather than a single narrow optimum.

The false down-weighting rate in this region ranged from 2.6% at $\beta = 0.08$ to 0.5% at $\beta = 0.20$, demonstrating a smooth tradeoff between transient attenuation strength and nominal diagnostic influence.

These results indicate that the DSFB weighting structure exhibits stable transient attenuation behavior over a non-trivial parameter region in the simulated scenario.

6.10 Simulation results

Figure 1 shows reconstruction error trajectories under the injected ELM-like transient corruption. Equal weighting produces a peak error of 0.4576. DSFB adaptive weighting (illustrated here at $\alpha = 1.2$, $\beta = 0.1$) reduces the peak to 0.3915, corresponding to a 14% reduction relative to equal weighting. Covariance inflation and Huber IRLS achieve lower peak amplitudes (0.1530 and 0.1436 respectively), but at the cost of either sustained nominal suppression (covariance inflation) or increased computational burden (IRLS).

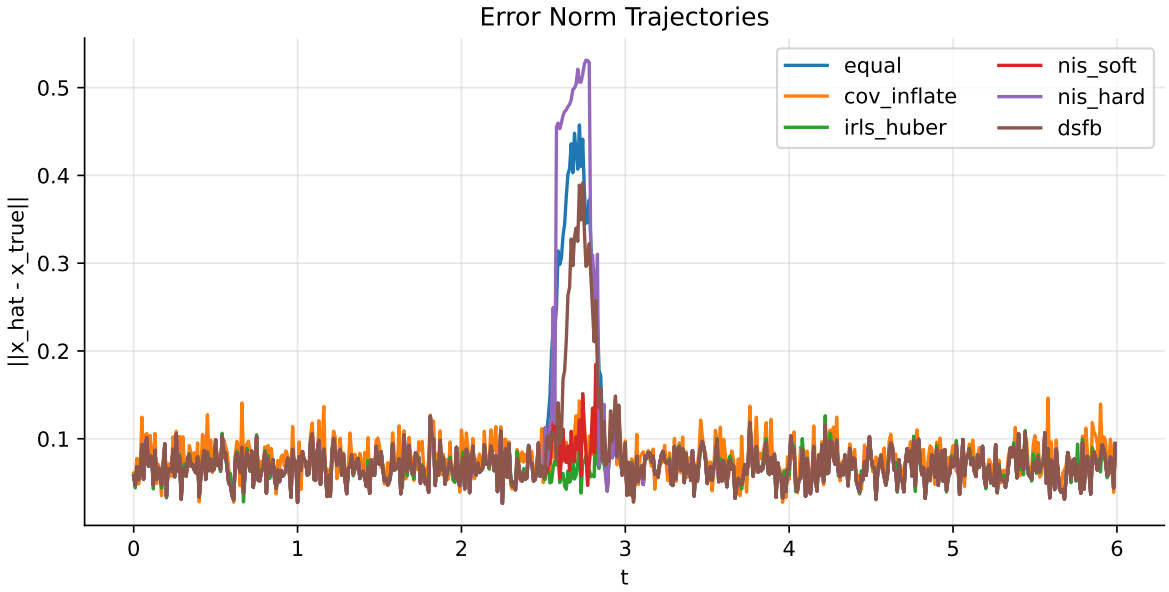

Figure 1: Reconstruction error norm trajectories for all evaluated methods under injected transient corruption.

Figure 2 compares trust-weight evolution for DSFB and soft NIS gating. DSFB weights decrease smoothly during the disturbance interval, reaching minimum values between approximately 0.1 and 0.2, and recover continuously thereafter. In contrast, NIS-based attenuation exhibits sharper and more discontinuous suppression behavior. No hard diagnostic rejection occurs under DSFB.

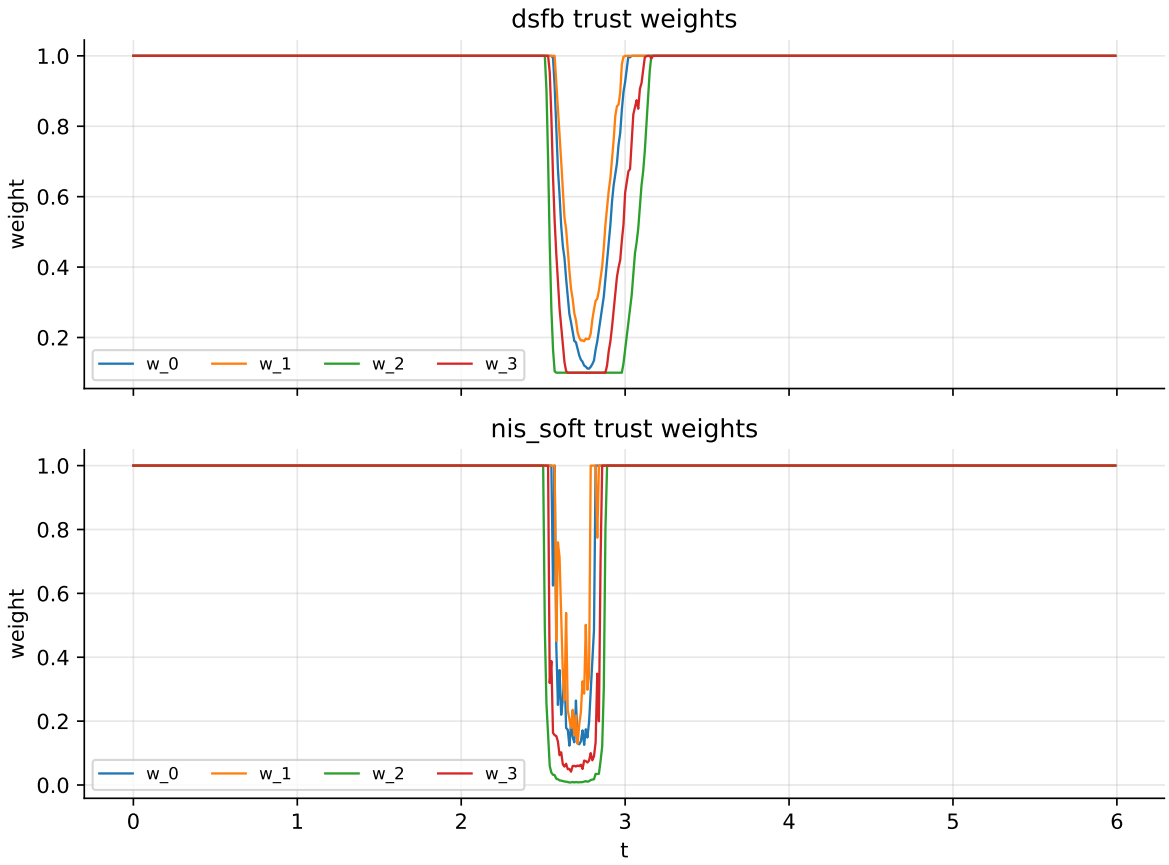

Figure 2: Trust-weight evolution for DSFB and soft NIS gating during transient corruption. DSFB exhibits smooth attenuation and recovery without hard rejection.

Figure 3 presents peak reconstruction error over the (α, β) parameter grid. A broad low-error region is observed near $\alpha = 0.4$. The minimum peak error within the evaluated grid occurs at $\alpha = 0.4$, $\beta = 0.08$, yielding $\max_t \|\hat{x} - x_{\text{true}}\| = 0.1997$. Relative to equal weighting (0.4576), this corresponds to a 56% reduction. Performance degrades gradually as α increases, indicating reduced envelope responsiveness to transient corruption.

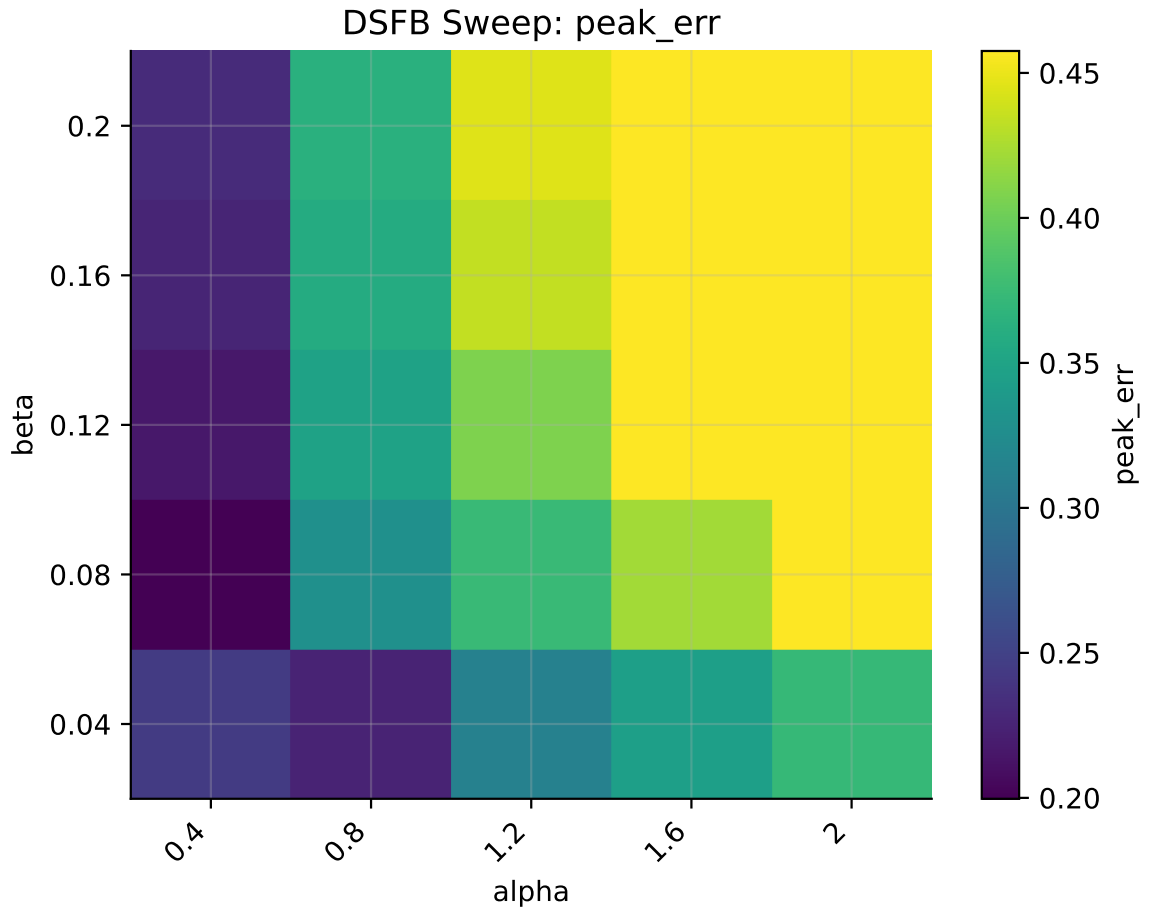

Figure 3: Peak reconstruction error over the (α, β) parameter grid. A broad low-error region is observed near $\alpha = 0.4$, with minimum peak error at $\alpha = 0.4$, $\beta = 0.08$.

Figure 4 shows the corresponding false down-weighting rate during nominal (non-corrupted) intervals. For $\alpha = 0.4$, false suppression decreases smoothly from 2.6% at $\beta = 0.08$ to 0.5% at $\beta = 0.20$. This demonstrates a controllable tradeoff between transient attenuation strength and nominal diagnostic influence.

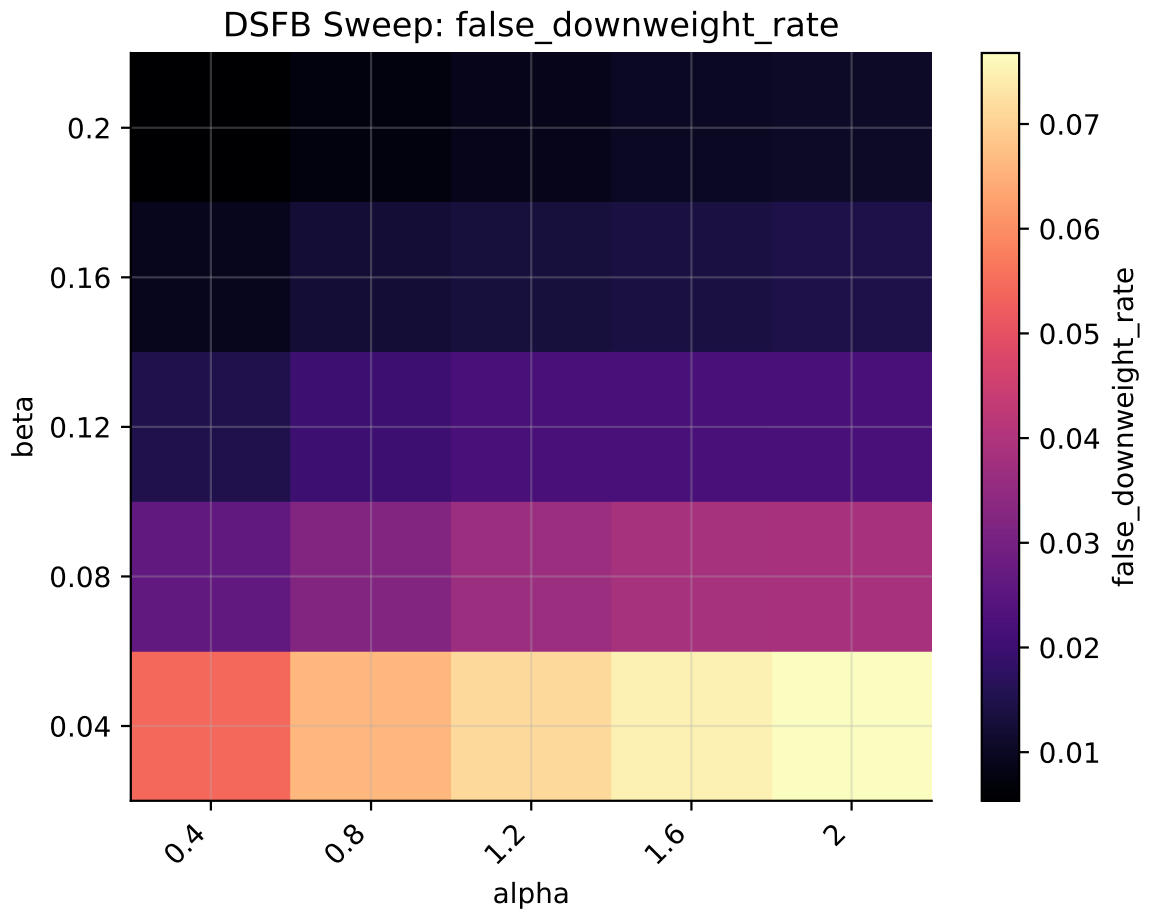

Figure 4: False down-weighting rate during nominal intervals. Increasing β reduces nominal suppression, illustrating a smooth tradeoff between attenuation strength and diagnostic preservation.

These results indicate that DSFB provides substantial transient attenuation relative to equal weighting, while maintaining continuous and tunable diagnostic influence outside corruption intervals.

7 Practical Deployment Considerations

The proposed adaptive trust weighting mechanism is intended as a minimal architectural extension to existing reconstruction systems. This section discusses implementation aspects relevant to real-time and offline deployment in magnetic confinement experiments.

7.1 Computational overhead

The additional computation introduced by the DSFB layer consists of:

- Residual computation $r_k = y_k - H_k\hat{x}$ for each diagnostic,
- Scalar envelope update per diagnostic,
- Scalar weight multiplication in the normal equation assembly.

For a system with total measurement dimension $M = \sum_k m_k$, residual computation scales as $\mathcal{O}(M)$. Envelope and weight updates are $\mathcal{O}(K)$ operations, where K is the number of diagnostic groups. These operations are negligible compared to matrix assembly and inversion costs typically associated with equilibrium reconstruction.

No additional matrix factorizations or iterative solvers are required beyond those already present in weighted least-squares implementations. As such, the method is compatible with real-time reconstruction cycles operating at sub-millisecond time scales.

7.2 Integration into existing pipelines

The adaptive trust layer can be incorporated at the stage where diagnostic weighting is applied in the normal equations. In systems similar to EFIT-style reconstruction:

- The computation of sensitivity matrices H_k is unchanged.
- The physics constraints and regularization terms remain intact.
- Only the diagnostic weighting factors are modified dynamically.

Implementation therefore requires minimal modification of solver infrastructure. In many cases, it is sufficient to insert multiplicative scaling factors in the existing diagnostic weighting matrices.

7.3 Parameter selection

The envelope memory parameter α determines the effective time constant of trust adaptation. Smaller values produce faster response to transient residual growth but may increase sensitivity to noise. Larger values produce smoother weight evolution with slower recovery.

The sensitivity parameter β determines the degree of attenuation for a given residual magnitude. A practical tuning strategy is to normalize residual magnitudes by nominal noise levels and select β such that moderate deviations produce limited attenuation, while extreme deviations produce substantial down-weighting.

Parameter selection does not require event-specific thresholds and may be performed offline using representative discharge data.

7.4 Numerical stability considerations

Because $w_k \in (0, 1]$, adaptive weighting reduces the effective contribution of selected diagnostics but does not introduce negative weights or sign changes. To ensure numerical robustness in edge cases, a lower bound $w_k \geq w_{\min} > 0$ may optionally be enforced. This prevents complete elimination of any diagnostic from the reconstruction and preserves conditioning of the normal equations.

7.5 Compatibility with advanced reconstruction methods

Although demonstrated here within a weighted least-squares framework, the trust-adaptive weighting structure is compatible with:

- Regularized reconstruction with Tikhonov terms,
- Iterative solvers and constraint-based formulations,
- Hybrid deterministic–stochastic reconstruction approaches.

The DSFB layer modifies only the relative contribution of measurement residuals and does not impose assumptions on the underlying plasma model.

7.6 Operational interpretation

From an operational perspective, the adaptive weights provide a continuously varying measure of diagnostic consistency. This may offer additional diagnostic health insight during high-activity phases, although such usage is outside the scope of the present study.

The primary function remains reconstruction robustness rather than diagnostic fault detection.

7.7 Runtime evaluation

Runtime performance was evaluated for the synthetic configuration ($K = 4$, total measurement dimension $M = 22$, state dimension $n = 8$) using a compiled implementation.

The baseline weighted least-squares solve required approximately 0.66 μs per reconstruction cycle. The DSFB envelope and trust update introduced an additional 0.89 μs per cycle, for a total of approximately 1.55 μs.

Thus, the adaptive trust layer increases per-cycle computation from 0.66 μs to 1.55 μs ($\approx 2.3\times$ relative to baseline WLS), while remaining below 2 μs per cycle in the tested configuration. For comparison, the iterative Huber IRLS baseline required approximately 5.62 μs per cycle under the same conditions.

No additional matrix factorizations or iterative solvers are introduced by the DSFB layer.

7.8 Reproducibility

All simulation code, parameter files, and plotting scripts are released with fixed random seeds to enable exact reproduction of the reported figures. A reference implementation is provided as both a notebook workflow and a compiled implementation suitable for integration testing.

A reference implementation is provided in a compiled language to demonstrate real-time feasibility and deterministic performance, alongside a notebook implementation for reproducibility.

Reproducibility artifacts, including raw simulation outputs and configuration files, are archived alongside this publication on Zenodo.

8 Limitations

Several limitations of the present study should be noted.

First, the simulation study is synthetic and does not incorporate experimental tokamak data. While the disturbance injection is designed to emulate ELM-like transient corruption, validation on real diagnostic datasets is required to assess performance under device-specific noise characteristics and plasma behavior.

Second, parameter selection for the envelope memory (α) and attenuation sensitivity (β) influences adaptation speed and attenuation strength. Although tuning does not require event-specific thresholds, suboptimal parameter choice may either over-attenuate nominal diagnostics or under-attenuate transient corruption. Practical deployment would benefit from calibration against representative discharge data.

Third, the method does not replace stochastic filtering or full probabilistic state estimation frameworks. It operates as a deterministic trust modulation layer applied to existing reconstruction equations. In scenarios where model uncertainty dominates measurement error, adaptive weighting alone may not address reconstruction inaccuracies.

Fourth, the approach assumes that residual magnitude is an informative indicator of diagnostic inconsistency. In cases where model mismatch or unmodeled plasma physics produces coherent multi-diagnostic residual growth, adaptive down-weighting could reduce sensitivity to genuine physical evolution. Careful interpretation of residual structure is therefore necessary.

Finally, the present formulation does not explicitly model correlated diagnostic errors. Extensions incorporating residual correlation structure may further refine trust adaptation, but are beyond the scope of this work.

Despite these limitations, the adaptive trust architecture provides a practical mechanism for reducing transient diagnostic influence without modifying the underlying plasma model.

9 Conclusion

This work has presented the application of Drift–Slew Fusion Bootstrap (DSFB) as a trust-adaptive weighting layer for multi-diagnostic plasma state estimation in magnetically confined systems. The method introduces per-diagnostic residual envelopes and continuous trust weights that modulate measurement influence within standard weighted reconstruction formulations.

Unlike fixed weighting or static covariance tuning, the adaptive structure responds dynamically to residual growth associated with drift, bandwidth mismatch, and impulse corruption. Analytical scaling arguments show that extreme transient disturbances exhibit bounded influence under the trust weighting structure. A conceptual simulation study illustrates bounded transient influence during ELM-like corruption while preserving nominal diagnostic influence outside transient intervals.

The DSFB layer does not alter the plasma state parameterization, sensitivity matrices, or physical constraints of the reconstruction process. Its computational overhead is negligible relative to existing solver operations, and integration into established pipelines requires only modification of diagnostic weighting factors.

The objective of this work is not to replace equilibrium solvers or claim resolution of disruption-scale phenomena. Rather, it proposes a conservative architectural modification that improves robustness to transient diagnostic anomalies while maintaining compatibility with current plasma reconstruction practice.

Future work will focus on validation using experimental tokamak datasets and evaluation within real-time reconstruction environments.

References

[1] L. L. Lao, H. St. John, R. D. Stambaugh, A. G. Kellman, and W. Pfeiffer, "Reconstruction of current profile parameters and plasma shapes in tokamaks," *Nuclear Fusion*, vol. 25, no. 11, pp. 1611–1622, 1985.

[2] L. L. Lao, J. R. Ferron, R. J. Groebner, W. Howl, H. St. John, E. J. Strait, and T. S. Taylor, "Equilibrium analysis of current profiles in tokamaks," *Nuclear Fusion*, vol. 30, no. 6, pp. 1035–1049, 1990.

[3] J. R. Ferron, L. L. Lao, E. J. Strait, and T. S. Taylor, "Real-time equilibrium reconstruction for tokamak discharge control," *Nuclear Fusion*, vol. 38, no. 7, pp. 1055–1066, 1998.

[4] S. C. Jardin, *Computational Methods in Plasma Physics*, CRC Press, 2012.

[5] D. A. Humphreys *et al.*, "Advances in equilibrium reconstruction for plasma control," *Nuclear Fusion*, 2015.

[6] H. Zohm, "Edge localized modes (ELMs)," *Plasma Physics and Controlled Fusion*, vol. 38, no. 2, pp. 105–128, 1996.

[7] R. de Beer, "Slew-Aware Trust-Adaptive Nonlinear State Estimation for Oscillatory Systems With Drift and Corruption (v1.0)," *Zenodo*, 2026. DOI: `https://doi.org/10.5281/zenodo.18642887`